RESEARCH ARTICLE | OCTOBER 06 2023

Aim point management system

Laurin Oberkirsch; David Zanger; Daniel Maldonado Quinto; Peter Schwarzbözl; Bernhard Hoffschmidt

AIP Conf. Proc. 2815, 030014 (2023)
https://doi.org/10.1063/5.0148732

Aim Point Management System

Laurin Oberkirsch[a)], David Zanger, Daniel Maldonado Quinto, Peter Schwarzbözl and Bernhard Hoffschmidt

Institute of Solar Research, German Aerospace Center (DLR), Linder Höhe, 51147 Köln, Germany

[a)] Corresponding author: laurin.oberkirsch@dlr.de

Abstract. The main objective of an aim point management system is the safe operation of solar tower power plants at higher efficiencies than with conventional control techniques. To achieve this aim, aim point optimization is indispensable, even though it suffers from highly fluctuating environmental conditions such as cloud courses. Modern plants, equipped with measurement systems, can predict the cloud movements and measure flux density distributions on the receiver's surface. In this work, the aim point management system is coupled with these measurement systems. Moreover, it comprises a novel closed-loop aim point control technique that includes aim point optimization. Based on the variability of the clouds, the system selects a safe operation mode. Furthermore, the system's modelling error is reduced by including the measurements. Finally, the feedback of the flux density distribution allows the controller to react on disturbances. In this work, the aim point management system is successfully tested at the solar tower in Jülich. There, the controller reacts on sudden changes in the allowable flux density within two to three control steps, each requiring ten seconds.

INTRODUCTION

The application of aim point optimization has a great potential in the control of solar tower power plants. They enable the plant to operate at higher plant efficiencies and simultaneously to comply with temperature and stress limits [1]. Despite the large potential, those techniques are seldom used in commercial facilities caused by two main reasons:

- Aim point optimization as open-loop control cannot compensate for modelling errors in the system model.
- Aim point optimization has usually no information about disturbances such as clouds moving across the sky above the heliostat field. These disturbances cause unexpected variations in the local Direct Normal Irradiance (DNI).

When controlling the plant under these highly fluctuating environmental conditions by aim point optimization, the risk for receiver damage and failure increases rapidly. As a result, most plants are still managed by human plant operators, who use conventional, quite conservative control techniques, even under clear sky conditions.

Nowadays, solar tower power plants can be equipped with measurement systems. On the one hand, All Sky Imager (ASI) based nowcasting systems can predict the DNI on the heliostat field for the near future [2]. On the other hand, the flux density on the receiver's surface can be measured [3, 4]. By combining aim point optimization with measurement data, higher efficiencies can be reached while minimizing the risk of receiver damages. An aim point management system accomplishes this combination.

After this introduction, an overview over a solar tower power plant including an aim point management system is provided. Subsequently, the coupled measurement systems and their interfaces as well as the interface to the field control system are described. Special focus lies on the processing of DNI maps and flux density distributions. Finally, first results at the solar tower in Jülich regarding the duration of a control step, the integration of DNI nowcasts and the applicability of a novel closed-loop aim point control are discussed.

SolarPACES: Solar Power & Chemical Energy Systems
AIP Conf. Proc. 2815, 030014-1–030014-8; https://doi.org/10.1063/5.0148732
Published by AIP Publishing. 978-0-7354-4623-6/$30.00

METHOD

The structure of a solar tower power plant, equipped with the aim point management system, is presented in Fig. 1. The power plant consists of a heliostat field, a receiver and a power block. At this system, several measurement systems are installed. Firstly, ASI based nowcasting systems generate DNI maps for the present as well as for the near future [2]. Secondly, flux density measurement systems determine the flux density distribution on the receiver's surface [3, 4]. Further measurement systems can also be installed, but are not part of this work. Here, an infrared (IR) camera determining the temperature distribution on the receiver's surface and temperature or mass flow sensors can be named. Additionally, deflectometry measurements help reducing and quantifying the modelling error for imperfect mirror reflectivity.

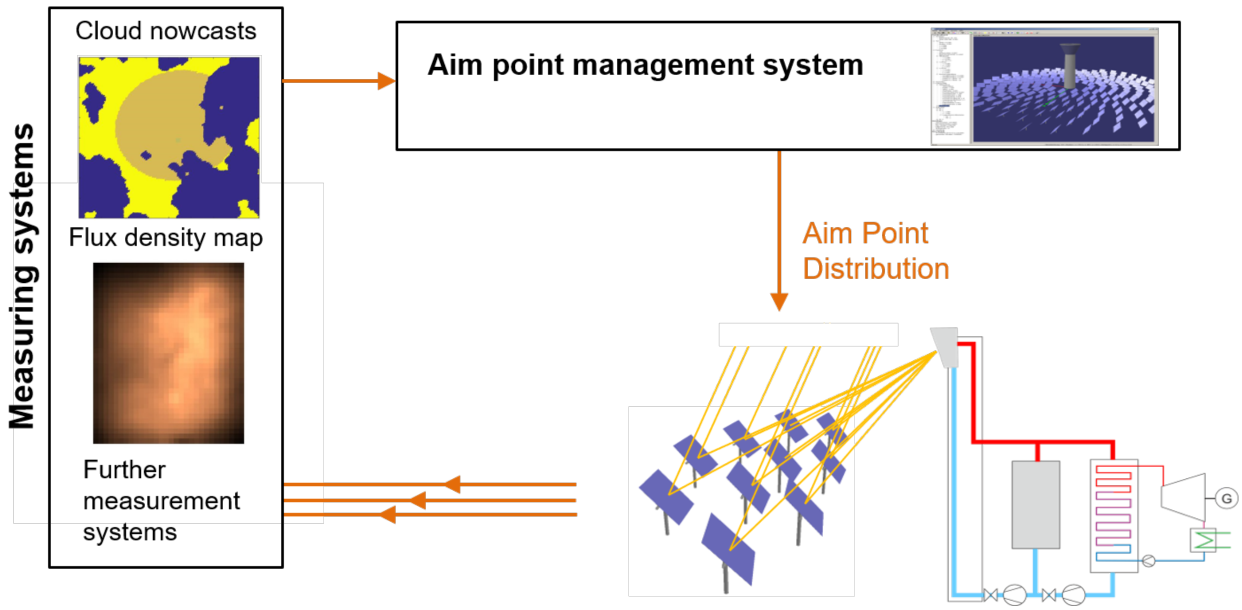

FIGURE 1. Embedding of the Aim Point Management System in the control of a solar tower power plant. Measurement data such as cloud nowcasts and flux density maps on the receiver are recorded at the plant and transferred to the aim point management system. The system, in turn, proposes based on the data an aim point distribution for the field control to set.

All measurement data are sent to the Aim Point Management System, which processes the data and determines with the help of aim point optimization and control algorithms a good aim point distribution. This distribution is requested by the field control to assign each heliostat to an aim point.

Measurement Systems

All Sky Imager

The All Sky Imager based nowcasting system embedded in this work creates an individual 3D model of each cloud by voxel carving. The clouds are tracked by assigning attributes like height, position, surface area, volume, transmittance and motion vector to each cloud. Finally, the nowcasting system generates spatially resolved DNI maps with a size of 8 km × 8 km for lead times up to 15 min. The DNI maps have a spatial resolution of 20 m × 20 m and a temporal resolution of 1 min [5]. Moreover, upper and lower uncertainty values representing 68.3% coverage probability are derived from historical data [6].

Flux Density Measurement System

The Flux Density Measurement System records the reflected radiation from the absorber by a digital camera. In comparison to other flux density measurements, no special hardware like moving bars is required. Initially, the images are deskewed and unwinded to create a flat image of the concave receiver surface. Subsequently, an intensity value is detected for each absorber cup. Moreover, ambient light correction and bidirection reflectance function correction are applied [4]. Further advancements of this method are conducted by Offergeld et al. [3]. They also considered the relative absorber's reflective properties determined by the Scan Method and the effect of heliostats irradiating from different heliostat field areas.

Aim Point Management System

The *Aim Point Management System* is embedded in the raytracing software STRAL. The Solar Tower Raytracing Laboratory (STRAL) is a raytracing software tool developed at the German Aerospace Center [7]. It comprises *Aim Point Management* itself, *Cloud Data Analyzer* and *Aim Point Control* as shown in Fig. 2. Each subsystem is included as a toolbox.

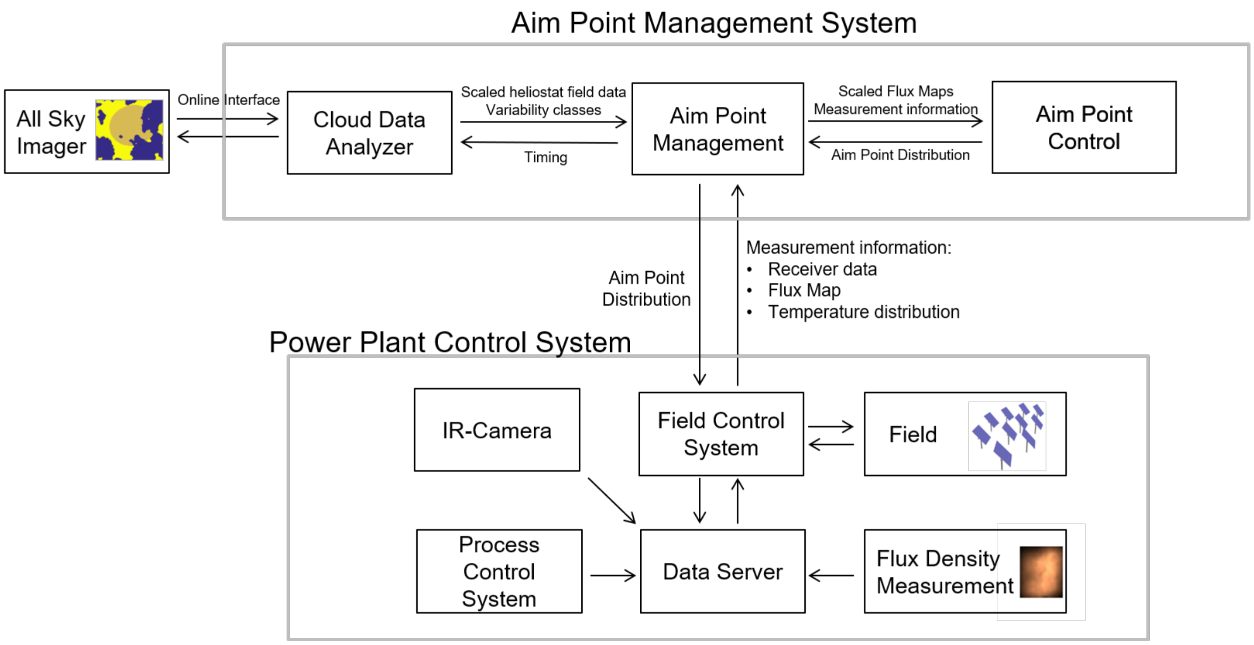

FIGURE 2. Aim Point Management System including its subsystems Cloud Data Analyzer, Aim Point Management and Aim Point Control. The Aim Point Management System communicates with the All Sky Imager and the Power Plant Control System, which contains the measurement systems, the Field Control System and the heliostat field itself.

Cloud Data Analyzer

The Cloud Data Analyzer includes a communication interface to the DNI nowcasting system via the Transmission Control Protocol/Internet Protocol (TCP/IP). Here, it functions as client and the nowcasting system as server. Implemented are commands for starting and aborting the system. Moreover, clear sky DNI and information about all available DNI maps in a certain time range can be requested. If no DNI maps are available or the TCP/IP connection is lost, an error is thrown. Otherwise, a decision regarding the most relevant DNI map is made based on the available DNI maps. Afterwards, the chosen DNI map, either the current one or the one of a specific time stamp, is requested. Based on this DNI map, a DNI is assigned as a feed-forward control to each heliostat. For this, the DNI map is mapped onto the area of the power plant's heliostat field.

Moreover, each heliostat produces a flux map on the receiver, when pointing to a certain aim point. These flux maps are pre-calculated by the system model in the raytracer STRAL and stored. They contain an accurate model of the power plant including various kinds of errors such as tracking errors. During optimization, the flux maps are loaded and also scaled with the predicted DNI information of the corresponding heliostats.

Additionally, the DNI maps of the subsequent ten minutes are used to analyze different cloud scenarios systematically. Each scenario is categorized in a distinct spatial and temporal variability class. The spatial classification is realized as described by Nouri et al. [2]. It uses the shadow area fraction S_A and shaded clear sky index S_i. The shadow area fraction is the quotient of shaded solar field area and complete solar field area. The shaded clear sky index is the quotient of average DNI in shaded areas and the clear sky DNI. The temporal classification is inspired by the procedure outlined by Schroedter-Homscheidt et al. [8]. They apply the clear sky index k_c, which is the quotient of DNI to clear sky DNI, and the number of changes in the sign of first derivative (CSFD). Here, a CSFD only counts, if the difference between two extrema exceeds 13%. This procedure is slightly adapted, since predictions for the next minutes instead of measurements of the past minutes are used.

Aim Point Management

The Aim Point Management is the heart of the Aim Point Management Systems. It includes Time and Sun Management, Pre-calculated Data Handler, Cloud Data Handler and Datalogger.

Main role of the Time and Sun Management is to update the system's internal time and to calculate and set dynamically the sun angles, elevation and azimuth, of the simulation model. Additionally, it determines the sun course of the next day and the downtime of the plant during the night.

The Pre-calculated Data Handler manages the pre-calculated flux maps necessary for aim point optimization. To keep the modelling error arising from differences between actual sun angle and the one of the pre-calculated flux maps below 1%, the difference between the sun angles should not exceed 1° in elevation and azimuth direction [9]. To achieve this coverage, the Pre-calculated Data Handler requires the next day's sun course from the Time and Sun Management. Moreover, the Pre-calculated Data Handler determines the number of pre-calculations that can be executed during the night. For this, it divides the plant's downtime by the time required for a single pre-calculation. For each pre-calculation, the sun angles in the raytracer STRAL are adjusted. After pre-calculation, the pre-calculated flux maps are written into a database. When starting the Aim Point Management System, the Pre-calculated Data Handler reads the database to find out which flux maps are already available. During optimization, the Pre-Calculated Data Handler selects based on the current sun angle the closest pre-calculated flux maps in the database. Subsequently, they are loaded. In this way, the optimizer always works with flux maps with a low deviation from the actual sun angle.

The Cloud Data Handler communicates with the Cloud Data Analyzer. It requests the available DNI maps for the next minutes to decide which DNI map should be mapped onto the heliostat field for optimization or controlling purposes. Moreover, it selects an operation mode based on the spatial and temporal variability class. For this, a characteristic diagram is defined. Possible operation modes are *Off*, *Conventional Control*, *Aim Point Control* and *Aim Point Optimization*. If complete overcast conditions occur, the plant is turned off. If clear sky conditions are predicted for the next minutes, the aim point optimization is used to maximize the plant's efficiency. If the modelling error in the simulation model rises or the DNI becomes more variable, closed-loop aim point control is used to minimize the modelling error with feedback information. The *Conventional Control* is proposed, if the cloud situation becomes more turbulent and no safe operation with the closed-loop aim point control can be guaranteed any longer.

Finally, the Datalogger logs all measurement data, variability classes and control parameters. The data is important to tune the control parameters and the characteristic diagram determining the operation mode.

Aim Point Control

In the Aim Point Control, the ant-colony optimization meta-heuristic (ACO) developed by Belhomme et al. [10] is applied as aim point optimization technique. This open-loop control method maximizes the intercept for arbitrary receiver shapes, while complying with the limits given by the allowable flux density. For this, the ACO superposes the with the raytracer STRAL pre-calculated flux maps. For the application in dynamic environments, Oberkirsch et al. [9] reduced the optimization duration. For this purpose, next to the use of pre-calculated flux maps, a grouping strategy is applied and the algorithm is implemented on a Graphics Processing Unit (GPU) to exploit its parallelization potential.

To close the control-loop, a control approach called *Static Optimal Control* is developed by Zanger et al. [11] and included as closed-loop aim point control technique in the Aim Point Control toolbox. This closed-loop technique uses the feedback of the flux density measurements and determines the error between an optimized reference flux map and the measured flux map. Subsequently, a weight estimator updates weights that are included in the cost function of an aim point optimizer based on this error. In this way, the feedback is included in the optimization, since the optimizer prefers aiming at points with higher weights and reduces the flux at points with low weights. The ACO is employed as aim point optimizer to profit of the previously mentioned improvements.

Power Plant Control System

The individual components of the Power Plant Control System and its interfaces are pictured in Fig. 2. Here, the infrared (IR) camera determines the temperature distribution. The Process Control System measures further receiver data like temperatures or mass flows with temperature and mass flow sensors. Additionally, the flux density measurement system determines the flux density distribution on the receiver's surface. All these measurement data of the power plant are sent to a Data Server. There, the systems act as clients sending the data to the server. The flux density and temperature measurements are matrices with 36 x 30 entries. Each entry describes a measuring point for one absorber cup of the open volumetric receiver installed at the solar tower in Jülich. The additional receiver data are scalar values, which are measured e.g. at different temperature or mass flow sensors within the receiver.

The Field Control System acts as client in connection with the Data Server and queries the current data. This data is subsequently forwarded to the Aim Point Management. The connection between Field Control System and Aim Point Management is realized via a TCP/IP, where the Field Control System is the client and the Aim Point Management is the server. Furthermore, the Field Control System also starts and terminates the aim point management system and sends a list of available heliostats. At the same time, it queries the aim point distribution from the Aim Point Management, which reads this information from the Aim Point Control. Afterwards, each active heliostat is assigned to its aim point according to the received aim point distribution. For this, the Field Control System communicates with the controllers of the individual heliostats. If the connection to the aim point management system is lost, the heliostats are defocused, so that no unintentional flux or temperature overshoots emerge. Additionally, the Field Control System triggers defocus events, if temperature limits or limits of the temperature gradient are overstepped.

RESULTS AND DISCUSSION

First, a quick overview over the different test phases of the aim point management system conducted at the solar tower in Jülich is given. Afterwards, the duration of a single control step is deduced, before the aim point management system is analyzed. Here, special focus lies on the inclusion of DNI nowcasts and on the closed-loop aim point controller using the flux density measurements.

The solar tower in Jülich has a height of 60 m and an open-volumetric receiver with 36 x 30 absorber cups is mounted at the top. Each absorber cup has a size of 14 x 14 cm² and there are 0.5 cm gaps in between the cups. For the tests of the aim point management system, 120 aim points plus two additional off-receiver aim points are selected. The aim points are chosen, so that each aim point is in the middle of nine neighboring absorber cups.

Test Phase 1

During the first test phase, the individual interfaces and their commands have been successfully tested at the solar tower in Jülich on eleven test days in September 2020. During this time, aim point optimization and closed-loop aim point control have been examined individually. Here, closed-loop aim point control showed better results than aim point optimization. Reasons for the worse results of the aim point optimization are deviations between the simulation model and the reality. These errors are caused by errors in the DNI nowcast and by modeling errors such as incorrectly assumed tracking errors. The tracking errors could not be modelled sufficiently accurate as the tests are conducted with a small number of heliostats. In comparison to the aim point optimization, the closed-loop aim point control is able to compensate for these deviations by the using the provided feedback information. Hence, it achieves better results even under clear sky conditions.

For these first tests, a sample time of 30 seconds was used. The sample time was mostly determined by the time required by the heliostats to move. One reason for the slow heliostat movement is the low traverse speed of the heliostats as both axes had to drive one after another. A second reason is that the controllers miscounted the driven impulses. Thus, they drove too far and had to compensate for that error.

Test Phase 2 and Control Step

During the second test phase, six test days in spring 2021, 28 heliostats have already been equipped with new drives and controllers. Hence, they have been used to significantly reduce the sample time and thus, the duration of a control step. The total duration of a control step is divided into three periods: The time required by the algorithm, the time required by the heliostats to move and the time required by the measurement system to determine a new flux density distribution.

The time required by the algorithm is mostly characterized by the optimization duration. The longer the optimization, the better is the reached convergence. Oberkirsch et al. [9] studied the convergence of the ACO as aim point optimizer at a large scale 450 MW reference power plant. Using the grouping strategy and the GPU implementation, the ACO finds aim point distributions leading to a convergence of over 99.5% compared to the achieved maximum in roughly 10 seconds. Following these results, an optimization duration of roughly two seconds is totally sufficient to ensure a great convergence for the small number of heliostats utilized in this work.

The time required by the heliostats to move is mostly determined due to a timer within the Field Control System. The system sends new commands to the heliostat field only every five seconds to reduce the number of heliostat movements and in consequence degradation. Hence, heliostats are assigned just every five seconds to new aim points and on average it takes 2.5 seconds until the command is sent. The heliostats with the new drives are comparably fast as they can move both axes at once and the controller does not miscount the impulses any longer. Thus, they can move from one side of the small receiver to the other in one to two seconds depending on the distance to the tower. Adding both times leads to a minimal movement time of one second and a maximal time of seven seconds. On average, the movement takes roughly four seconds.

The time required by the flux density measurement system splits into three parts: The time between two pictures, the post-processing time and the time sending it to the Aim Point Management System. Here, the maximal time is estimated to two seconds, whereas the average time should be around one second.

Summing all durations, the control step should be at least twelve seconds to ensure that the heliostats are assigned to their new aim points and that the newly measured flux density belongs to this aim point distribution. However, most of the adaptions are already realized in ten seconds. So, this time is applied here to react slightly faster on disturbances.

Analysis of DNI Nowcasts

During all days of operation, the DNI maps as well as the determined spatial and temporal variability classes are logged. At the solar tower in Jülich, there is no conventional control strategy implemented. Moreover, the aim point optimization led to worse results than the closed-loop aim point control as already discussed. Thus, the operation mode *Aim Point Control* is tested most of the time, whereas the operation modes *Aim Point Optimization*, *Conventional Control* and *Off* are not or rather less used during the tests. Now, all minutes of operation have to be analyzed to fill the characteristic diagram for the operation modes for the solar tower in Jülich. For this, it has to be checked whether the application of the closed-loop aim point control would have been safe. Figure 3a provides an example for an unsafe operation period, since it could not be guaranteed that no overflux condition occurs. In this way, the hours of save operation and the critical hours will be determined for each combination of spatial and temporal variability classes to fill the characteristic diagram.

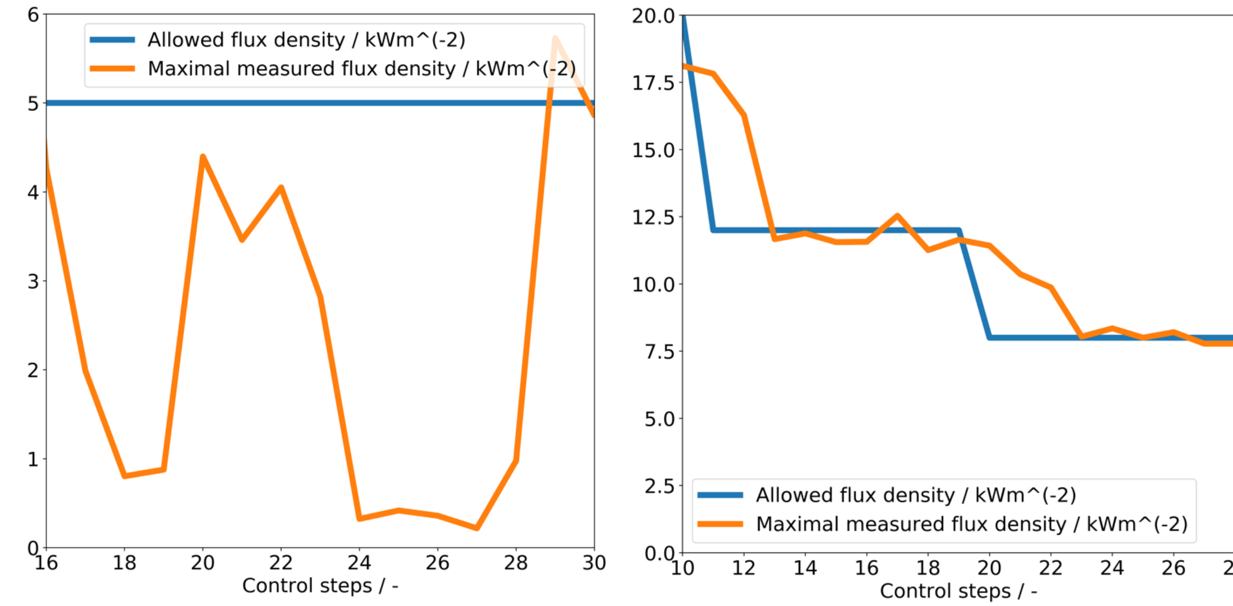

(a) (b)

FIGURE 3. Allowed flux density and maximal measured flux density. (a) The maximal measured flux density varies as clouds pass the heliostat field. (b) The allowed flux density setpoint is stepwise reduced. As a response, the closed-loop aim point control varies the aim point distribution, so that the maximal measured flux density complies with the new limit.

In Fig. 3a, the maximal measured flux density of 15 successive control steps is plotted. Since the maximal measured flux density is always below the allowed flux density, the closed-loop aim point control shifts all heliostats to centralized aim points to reduce spillage. Thus, the aim point distribution remains more or less constant in between and the differences in the maximal measured flux density are mostly caused by variations in the DNI irradiating on the used heliostats. Here, a control step requires also ten seconds. Hence, this exemplary time frame shows that clouds pass the small part of the heliostat field used in this work within 30 seconds up to one minute (3 to 6 control steps). Thus, the temporal resolution of one minute in the data of the All Sky Imager is not sufficiently accurate for the application in scaling of pre-calculated flux maps for optimization or controlling purposes at the solar tower in Jülich. Using the DNI maps, nevertheless, led to unexpected high fluxes on the receiver, if the nowcasting system predicts a cloud erroneously and there is none in reality. For greater systems with significantly larger heliostat fields, still an advantage of including the DNI forecasts in the optimization by scaling the pre-calculated flux maps is expected. However, it cannot be analyzed at the here tested system.

Analysis of Closed-Loop Aim Point Control

The closed-loop aim point control is already tested simulatively by Zanger et al. [11]. They studied how the controller compensates for cloud disturbances and modelling errors e.g. inaccurate modelled mirror errors. Here, the focus is on safety and how the controller reacts in reality. Thus, the closed-loop aim point control is tested by imprinting a stepwise reduction of the allowed flux density setpoint. Here, it is reduced from 20 kW/m², first to 12 kW/m² and later down to 8 kW/m² as shown in Fig. 3b. The maximal measured flux density reduces as a response, too. Thus, the closed-loop aim point control is able to find new aim point distributions observing the new flux density limit. However, a delay of two to three control steps corresponding to 20 to 30 seconds is detected. The control steps are needed by the closed-loop controller as the weight estimator slowly adapts the internal weights based on the error to prevent oscillations in the system. On basis of the adapted weights, the controller finds new aim point distributions complying with the new allowable flux density limit. As soon as the limit is met, the controller is stable. The small overstepping above the allowable flux density limit occurs only in single absorber cups. In these cases, the ratio of exceeded flux to total flux is always below 0.05%. This is considered as acceptable.

CONCLUSION

In this work, the aim point management system is introduced. The necessary interfaces to different measurement and control systems are implement and sufficiently tested at the solar tower in Jülich. DNI information predicted by an All Sky Imager are used to determine spatial and temporal variability classes. These classes will be used, so that aim point control is only applied, if the safety of the plant is guaranteed. The inclusion of the DNI information in the optimization itself could not be tested due to the limited size of the test plant. Moreover, a flux density measurement system provides feedback for a closed-loop aim point control. It is demonstrated that the controller can comply with varied setpoints of the allowable flux density limit within two to three control steps by using this feedback.

In future, the aim point management system will be tested with more heliostats to test also the embedding of DNI information in the optimization. Moreover, the other feedback information, temperature distribution and further receiver data, will be used by the aim point management system to control not only the flux density distribution, but also the temperature distribution.

ACKNOWLEDGEMENTS

This work was carried out in the project “HeliBo” (Grant No.: PRO0070 A) with the financial support from the Ministry of Economic Affairs, Innovation, Digitalization and Energy of the State of North Rhine-Westphalia.

REFERENCES

1. D. Maldonado Quinto, R. Flesch, A. Reinholz and P. Schwarzbözl, “Evaluation of aim point optimization methods” in *SolarPACES* 2017, AIP Conference Proceedings 2033, edited by R. Mancilla and C. Richter (AIP Publishing, Maryland, 2018), 040025, https://aip.scitation.org/doi/abs/10.1063/1.5067061.
2. B. Nouri, K. Noureldin, T. Schlichting, S. Wilbert, T. Hirsch, M. Schroedter-Homscheidt, P. Kuhn, A. Kazantzidis, L.F. Zarzalejo, P. Blanc, Z. Yasser, J. Fernández and R. Pitz-Paal, Solar Energy **198**, 434-453 (2020).
3. M. Offergeld, M. Röger, H. Stadler, P. Gorzalka and B. Hoffschmidt, “Flux density measurement for industrial-scale solar power towers using the reflection off the absorber” in SolarPACES 2018, AIP Conference Proceedings 2126, edited by C. Richter (AIP Publishing, Maryland, 2019), 110002, https://aip.scitation.org/doi/abs/10.1063/1.5117617.
4. F. Göhring, O. Bender, M. Röger, J. Nettlau and P. Schwarzbözl, “Flux density measurement on open volumetric receivers”, Proceddings of SolarPACES 2011, Granada, Spain, Sept. 20-23.
5. B. Nouri, P. Kuhn, S. Wilbert, C. Prahl, R. Pitz-Paal, P. Blanc, T. Schmidt, Z. Yasser, L. R. Santigosa and D. Heineman, “Nowcasting of DNI maps for the solar field based on voxel carving and individual 3D cloud objects from all sky images” in SolarPACES 2017, AIP Conference Proceedings 2033, edited by C. Richter (AIP Publishing, Maryland, 2018), 190011, https://aip.scitation.org/doi/abs/10.1063/1.5067196.
6. B. Nouri, S. Wilbert, P. Kuhn, N. Hanrieder, M. Schroedter-Homscheidt, A. Kazantzidis, L. Zarzalejo, P. Blanc, S. Kumar, N. Goswami, R. Shankar, R. Affolter and R. Pitz-Paal, Remote Sensing **11**(9), 1059 (2019).
7. B. Belhomme, R. Pitz-Paal, P. Schwarzbözl and S. Ulmer, Journal of Solar Energy Engineering **131**(3), 031002 (2009).
8. M. Schroedter-Homscheidt, M. Kosmale, S. Jung and J. Kleissl. Meteorologische Zeitschrift **27**(2), 161-179 (2018).
9. L. Oberkirsch, D. Maldonado Quinto, P. Schwarzbözl, Bernhard Hoffschmidt, Solar Energy **220**, 1089-1098 (2021).
10. B. Belhomme, R. Pitz-Paal, P. Schwarzbözl, Journal of Solar Energy Engineering **136**(1), 011005 (2014).
11. D. Zanger, L. Oberkirsch, D. Maldonado Quinto and R. Pitz-Paal, “Static Optimal Control: A Closed-Loop Control Strategy for Heliostat Aiming in Solar Power Towers“ [Manuscript accepted for publication] in SolarPACES 2021.